JOURNAL OF CATALYSIS 111, 273–285 (1988)

Mixed Gels of Vanadia and Silica: Structural Properties and Catalytic Behavior in Selective Reduction of Nitric Oxide with Ammonia

A. BAIKER,[1] P. DOLLENMEIER, M. GLINSKI,[2] A. RELLER,[3] AND V. K. SHARMA

Department of Industrial and Engineering Chemistry, Swiss Federal Institute of Technology (ETH), CH-8092 Zürich, Switzerland

Received May 22, 1987; revised November 18, 1987

Mixed gel catalysts of vanadia and silica containing 0.1, 1, 10, 20, and 50 wt% of vanadia were prepared from alkoxides of the constituents. The catalysts were investigated with regard to their physical and chemical properties, and their activity in the selective catalytic reduction (SCR) of nitric oxide. The textural properties (grain morphology, BET surface area, specific pore volume, pore size distribution) were found to depend on the composition of the mixed gels and varied most strongly in the composition range 1–20 wt% of vanadia. Bulk structural and chemical properties were investigated by means of X-ray diffraction (XRD), high-resolution electron microscopy (HREM), electron spin resonance, and temperature-programmed reduction and oxidation. XRD and HREM revealed that silica was existing in all catalysts as an amorphous phase only. Vanadia showed more complex behavior. At low concentrations (less than 10 wt%) it consisted of well-dispersed vanadium oxide species, whereas at higher concentrations small microcrystalline domains were found in the amorphous V_2O_5 matrix. Highest specific activities (molecules of NO converted to N_2 per V^{5+} site per second) were measured for the catalysts containing 1 and 10 wt% of vanadia. Catalysts with higher vanadia contents exhibited a significant decrease in the activation energy around 430 K which is attributed to agglomeration of the well-dispersed vanadium oxide species under SCR conditions. The stability of the well-dispersed vanadium oxide species under SCR conditions was found to decrease with increasing temperature and vanadia content of the catalyst. In all mixed gel catalysts the well-dispersed vanadium oxide species were more stable than those in silica-supported vanadia layers.

INTRODUCTION

Recently considerable effort has been expended to gain more information about the structural and catalytic properties of silica-supported vanadia (*1–7*). It is generally agreed that the interaction of the vanadia species with the support is relatively weak in catalysts prepared by impregnation of silica with a vanadium-containing precursor (*1–4*). As a result of the weak interaction the immobilized vanadia species tend to agglomerate when exposed to higher temperatures. This behavior was shown recently for a silica-supported monolayer of vanadia during its use for selective catalytic reduction (SCR) of nitric oxide with ammonia (*8*). Agglomeration and formation of relatively large vanadia particles occurred at temperatures higher than about 430 K under SCR conditions. The agglomeration could be suppressed by using mixed gels of silica–titania as carrier instead of pure silica. The addition of titania to the silica matrix resulted in a strengthening of the vanadia–support interaction leading to a significant increase in the activity for SCR and to a markedly easier reduction of the immobilized vanadia species.

Here we report another approach for stabilizing finely dispersed vanadia species on silica. Vanadia is immobilized in the silica matrix by applying the sol–gel pro-

[1] To whom all correspondence should be addressed.

[2] On leave from the Polytechnical University of Warsaw, Poland.

[3] Institute of Inorganic Chemistry, University of Zürich, CH-8057 Zürich, Switzerland.

0021-9517/88 $3.00

cess. Mixed gels of vanadia and silica are prepared and investigated with regard to their structural and catalytic properties in SCR.

EXPERIMENTAL

Catalyst Preparation

Mixed gels of vanadia and silica were prepared from corresponding sols. The sols were prepared using the following procedures. For the vanadia sol; 100 g of freshly distilled vanadyl triisobutoxide (b.p. 379 K, 66 Pa) was added dropwise to 2 liters of stirred distilled water and the stirring continued for 30 min. Subsequently the isobutanol formed was removed by evaporation under reduced pressure at 323 K and a dark red V_2O_5 sol was obtained. For the silica sol, 208 g of distilled $Si(OC_2H_5)$ (b.p. 441 K, 100 kPa) was stirred with 0.5 liter of distilled water for 48 h at 323 K. Ethanol was then removed by evaporation under reduced pressure at 323 K and a colorless fully transparent silica sol was obtained.

Mixed gels containing 0.1, 1, 10, 20, and 50 wt% vanadia were prepared from the sols of vanadia and silica using the following procedure. First the prepared sols were diluted with distilled water to 1 liter volume, and then appropriate amounts of these diluted sols were mixed and stirred for 30 min. No precipitation was occurring under these conditions. Subsequently the mixed sols were dried at 333 K for 24 h and at 393 K for 72 h. After grinding the sieve fraction of 0.5 to 1-mm grains was calcined at 873 K.

The reference catalyst consisting of a vanadia layer on silica was prepared using the reaction of vanadyl triisobutoxide with surface hydroxyl groups of silica. The impregnation procedure has been described in detail in a previous report (*4*).

Catalyst Characterization

All catalysts were characterized by nitrogen adsorption (BET), X-ray diffraction (XRD), high-resolution electron microscopy (HREM), scanning electron microscopy (SEM), temperature-programmed reduction (TPR), temperature-programmed oxidation (TPO), and electron spin resonance (ESR) spectroscopy.

Pore size distributions were determined from the desorption branch of the measured hysteresis of the nitrogen adsorption at 77 K using the method of Pierce (*9*).

The apparatus used for the TPR and TPO measurements has been described in detail elsewhere (*10*). TPR profiles were obtained under the following conditions: flow rate, 1.25 ml/s (STP); reducing gas, 6% hydrogen in argon; heating rate, 0.167 K/s; sample weights were 300 mg for the supported vanadia layer, and 2 g, 500 mg, 365 mg, 182 mg, and 184 mg for the mixed gels containing 0.1, 1, 10, 20, 50 wt% of vanadia, respectively. TPO was carried out under similar conditions with 6% oxygen in argon as the oxidizing gas.

High-resolution electron microscopy of the samples was carried out using a JEOL 200CX microscope equipped with a tungsten filament and top-entry stage. All samples were finely ground and dispersed on a supported holey carbon film via a hexane/methanol slurry. Scanning electron micrographs were taken using a Philips SEM 525 instrument equipped with EDX facility. For the SEM and EDX studies agglomerates of the different materials were prepared on a conventional sample holder and covered with a gold film.

ESR spectra were recorded on a Varian E-line Century series spectrometer with 100 kHz magnetic field modulation. A Varian variable temperature accessory was employed for the measurements from 293 to 550 K.

Catalytic Activity Measurement

The apparatus used for activity measurements was described in detail in Ref (*11*). It consisted of a tubular continuous flow fixed-bed microreactor coupled with a quadrupole mass spectrometer serving as analyzer for NO, NH_3, H_2O, N_2O, O_2, and NO_2. Standard conditions were: total flow

rate, 2.08 ml/s (STP); catalyst load, 1 g; feed concentrations, 900 ppm NO, 900 ppm NH_3, 18,300 ppm O_2 in N_2.

RESULTS

1. Textural Properties

Textural properties of the mixed gels of silica and vanadia containing 0.1, 1.0, 10, 20, and 50 wt% vanadia are listed in Table 1. For comparison we also quote the corresponding properties of a catalyst prepared by immobilization of a vanadia layer on pure silica (*4*).

The BET surface area showed a maximum for catalysts containing about 10 wt% of vanadia mainly due to the existence of micropores besides the mesopores. Higher vanadia contents resulted in a drastic decrease in the surface area. Parallel to this decrease in the BET surface area we note the appearance of a new type of narrower mesopore; i.e., the originally monodisperse pore size distribution of the mesopores became bidisperse. Catalyst containing 1 wt% vanadia and less exhibited a monodisperse mesopore size distribution similar to that of pure silica with a most frequent pore radius of about 4 nm. The change from the monodisperse to the bidisperse pore size distribution is accompanied by a decrease in the mesopore volume of the catalysts. The silica-supported vanadia exhibited about the same BET surface area as the pure silica support. However, the pore volume as well as the most frequent pore radius of the impregnated silica was significantly smaller than that of the pure silica. This indicates that some textural changes occurred during impregnation and subsequent calcination.

TABLE 1

Textural Properties of Vanadia–Silica Mixed Gels and a Silica-Supported Vanadia Layer

Vanadia content (wt%)	Pore volume (cm^3/g)	Surface area (m^2/g)	Most frequent pore radius (nm)
0	0.76	256	4.0
0.1	0.74	262	4.0
1.0	0.74	311	4.0
10.0	0.44	506	3.8/2.0[b]
20.0	0.35	89	3.8/2.3[b]
50.0	0.14	50	3.8/1.9[b]
Si–V[a]	0.59	253	3.5

[a] Vanadia layer supported on silica.
[b] Maxima in bidisperse pore size distribution.

Samples with low vanadia contents (0.1 and 1 wt%) exhibited a rather smooth surface similar to that of pure silica. However, the grain and surface morphology changed markedly with increasing vanadia content. This is illustrated by comparing the top and bottom plates of Fig. 1 which show the grain morphologies of vanadia–silica mixed gels containing 0.1 and 50 wt%, respectively. The agglomerates in the samples with higher vanadia content (10, 20, 50 wt%) were made up of small particulate matter and as a consequence the surface was comparably rough. EDX measurements indicated that in all mixed gels the vanadia was homogeneously distributed within the silica matrix.

2. Bulk Structural Properties

X-ray diffraction patterns of the fresh (after calcination) vanadia–silica catalysts as well as of the pure silica are presented in Fig. 2. Catalysts containing 0.1, 1, and 10 wt% vanadia showed only a broad intensity maximum characteristic for amorphous solids. The catalysts with higher vanadia contents showed a broadened reflection around $2\theta = 7°$. A similar reflection was observed earlier in silica systems (*12*) and was attributed to the existence of small particles of a hydrated silica phase $SiO_2 \cdot 3H_2O$.

More information about the bulk structure and insight into the surface structure were obtained by HREM. Figure 3 shows that the pure silica agglomerates were made up of amorphous microparticles with diameters of 10–30 nm. Similar micrographs were obtained for catalysts containing 0.1 and 1 wt% vanadia, respectively. Electron diffraction of such samples showed no evidence for the formation of crystalline domains of vanadia. Accordingly no contrast

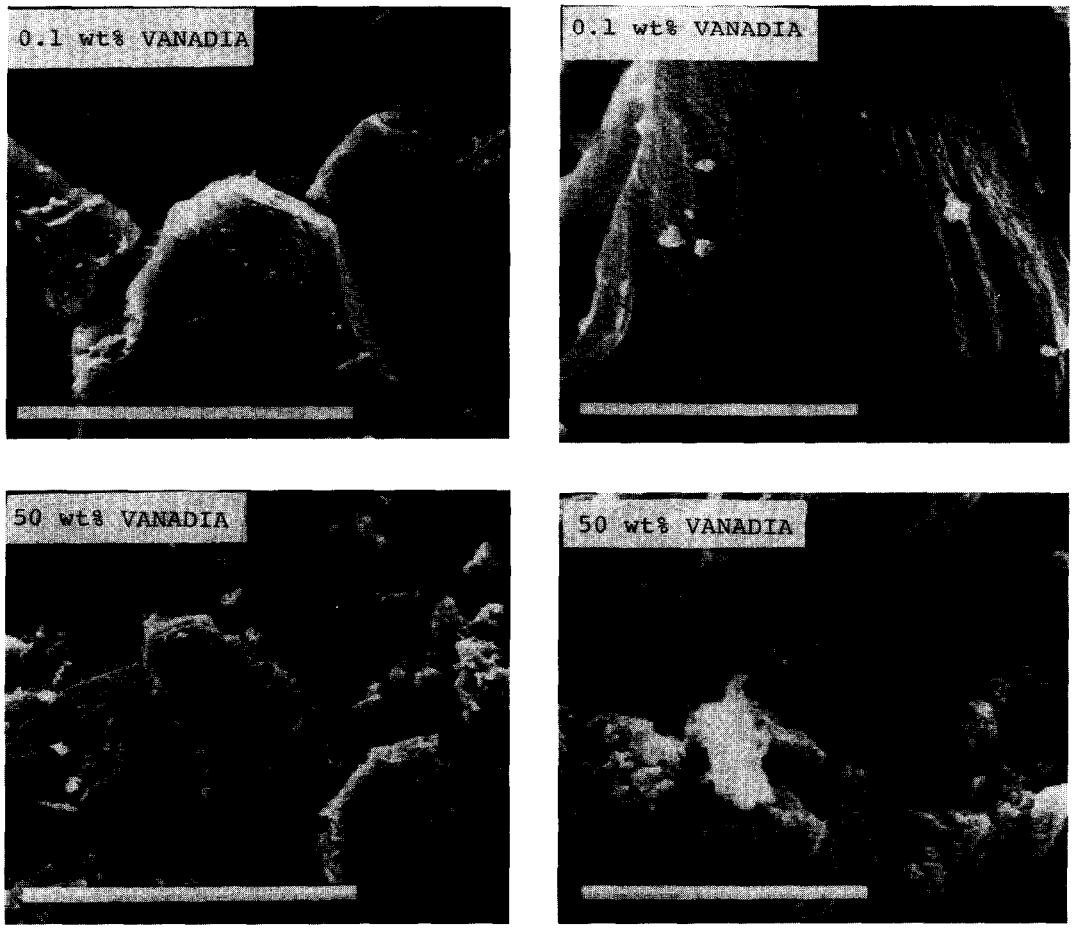

FIG. 1. Scanning electron micrographs showing the grain and surface morphologies of vanadia–silica catalysts with low vanadia content (top) and high vanadia content (bottom), respectively. The bars correspond to 0.1 mm (left plates) and 10 μm (right plates), respectively.

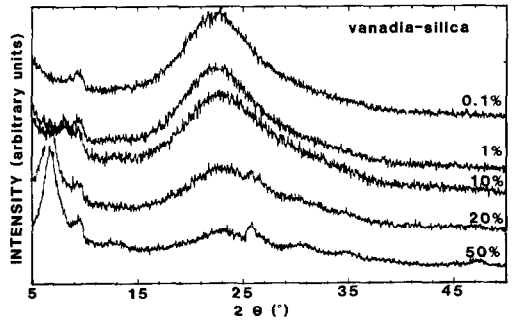

FIG. 2. X-ray diffraction pattern of vanadia–silica catalysts. Percentages quoted correspond to contents (wt%) of vanadia in mixed gels (CuK_α radiation).

maxima indicating arrays of concentrated vanadia could be observed in the high-resolution micrographs; i.e., vanadia was finely distributed within the silica matrix of these samples.

Vanadia also existed predominantly in the form of amorphous arrays in mixed gels containing 10 wt% vanadia (Fig. 4A). However, careful inspection of this material showed that a few domains of a crystalline vanadia phase have been formed. Characterization of these domains indicated that they contained microcrystalline V_3O_7 (*13*) and/or V_6O_{13} (*14*). Similar findings also emerge from the HREM investigation of

FIG. 3. High-resolution electron micrograph of pure silica sample.

the 50% vanadia–silica catalyst (Fig. 4B). Again small crystalline domains of the partly reduced vanadia phases are seen, but in much higher concentrations. The crystalline arrays appear to be very thin, with lateral dimensions of below 50 nm.

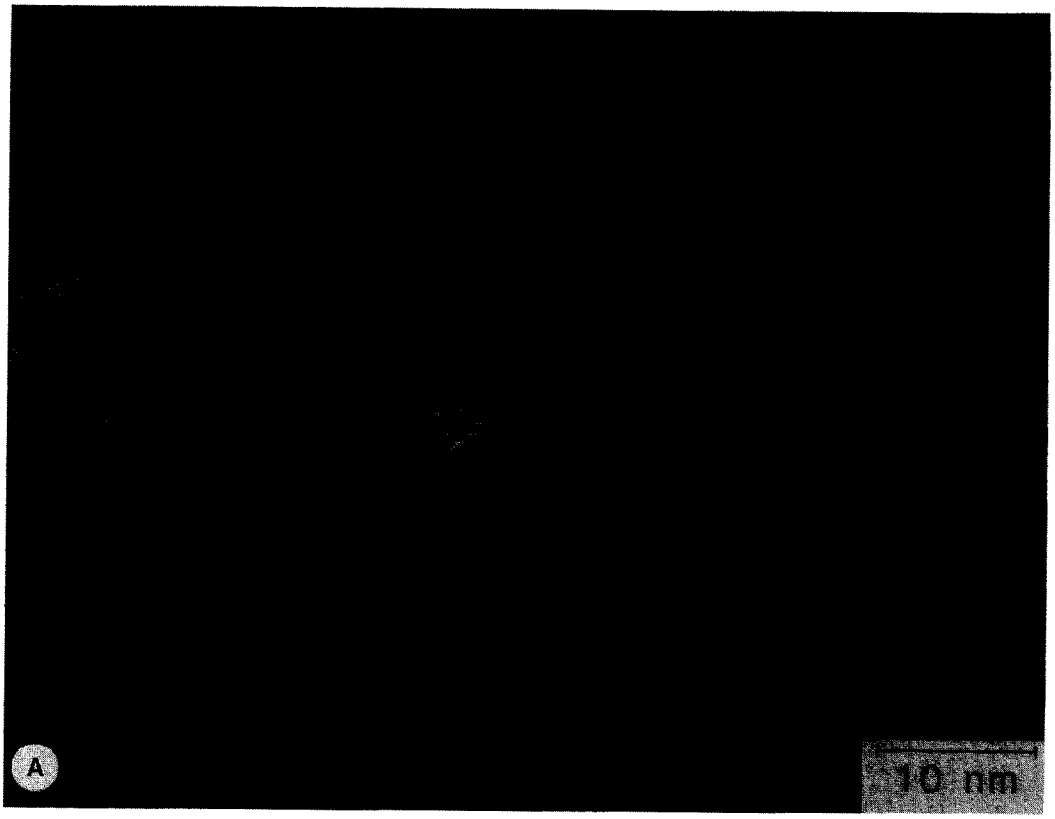

FIG. 4. High-resolution electron micrograph of vanadia–silica catalysts showing the microcrystalline domains of vanadium oxide embedded in the amorphous vanadia–silica matrix. (A) Vanadia (10 wt%)–silica catalyst. (B) Vanadia (50 wt%)–silica catalyst.

Temperature-programmed oxidation of the 50% vanadia–silica catalyst indicated that about 20% of the vanadia bulk was existing as partly reduced vanadia phases. HREM investigation of the 50% vanadia–silica sample after TPO revealed that the microcrystallinity of the partially reduced vanadia domains was restored during their transformation to V_2O_5. We note that neither the electron diffraction patterns nor the high-resolution electron micrographs indicated the presence of crystalline V_2O_5 in the fresh catalysts.

3. *Bulk Chemical Properties*

Electron spin resonance was used to gain information about the chemical structure of the vanadia species immobilized in the three-dimensional matrix of silica. The vanadian–silica catalysts containing 0.1 and 1 wt% vanadia exhibited very weak signals at room temperature indicating that only a small fraction of the vanadium ions was in the V^{4+} state. The ESR measurements of these samples were not extended to higher temperatures. Figure 5 depicts the ESR spectra recorded for vanadia–silica catalysts containing 10, 20, and 50 wt% vanadia. Samples containing 20 and 50 wt% of vanadia exhibit spectra similar to those reported for amorphous V_2O_5 after water vapor adsorption and for V_2O_5 xerogels which contain vanadium oxygen polymeric fibers (*15*). We can distinguish between three types of paramagnetic species: (i) well-dispersed VO^{2+} ions leading to the axial spectrum I (Fig. 5a) which is similar to the spectra measured for well-dispersed

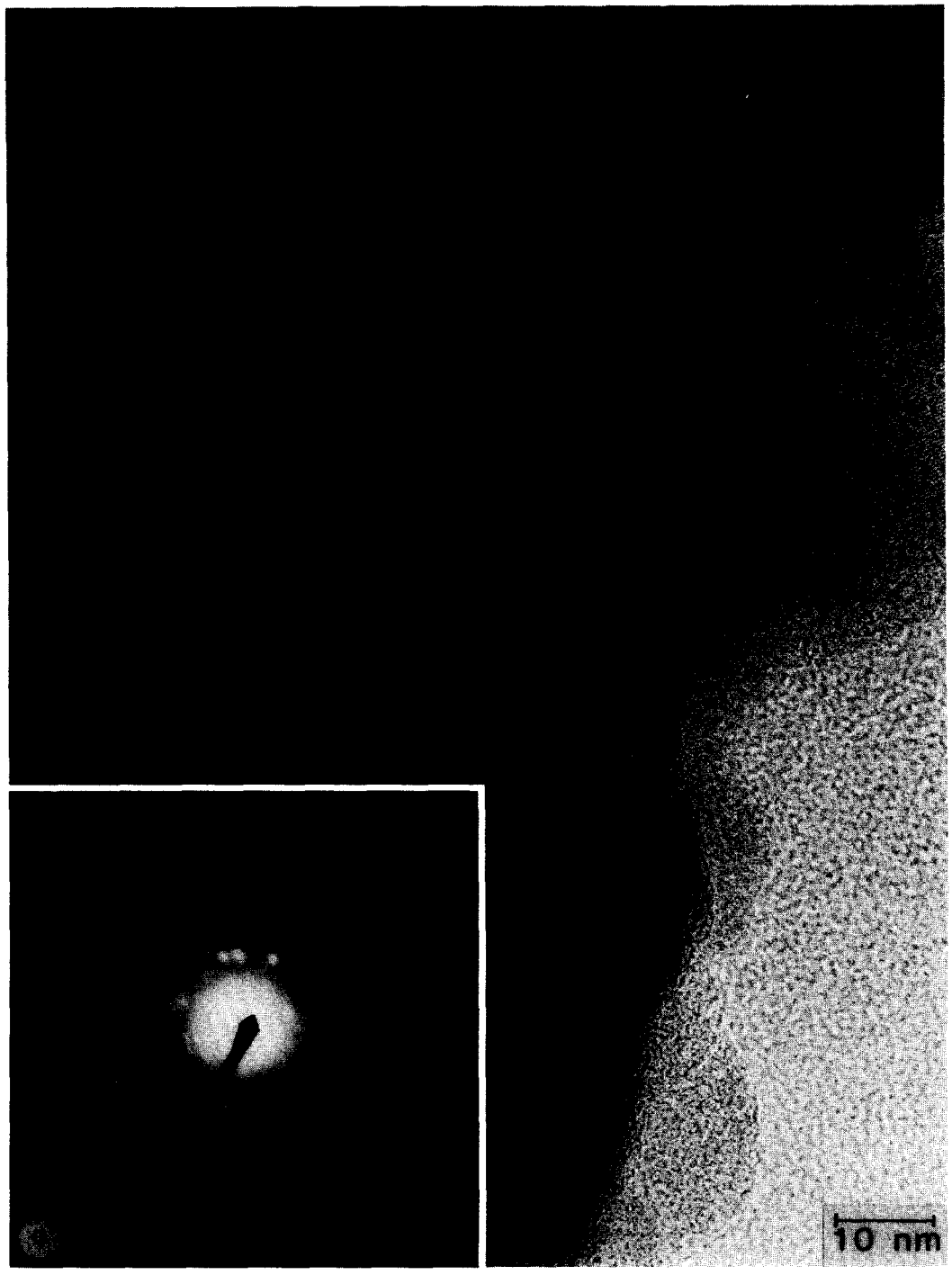

FIG. 4.—*Continued.*

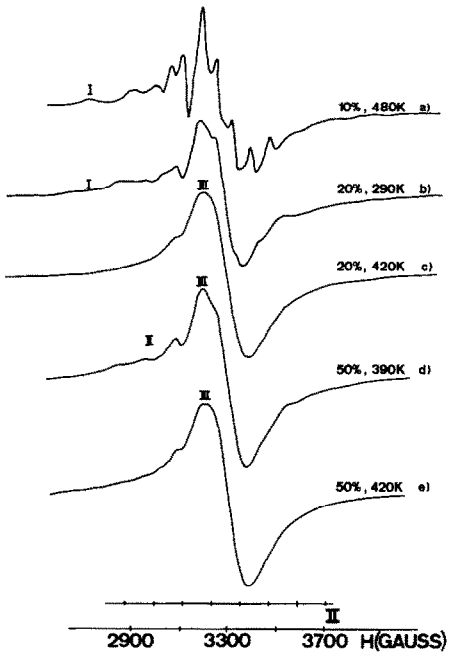

FIG. 5. ESR spectra of vanadia–silica catalysts containing 10, 20, and 50 wt% of vanadia. Spectra were recorded at the temperatures indicated.

supported vanadia monolayers (*16*); (ii) arrays of VO^{2+} species undergoing tumbling Brownian motion (*15*) characterized by spectrum II with an isotropic hyperfine constant A_0 = 121 G; and (iii) a microcrystalline phase reflected by spectrum III (Fig. 5c). The concentrations of the different vanadium oxide species change with increasing temperature.

The ESR signal of the sample with 10 wt% vanadia (Fig. 5a) consists predominantly of the well-dispersed VO^{2+} ions up to 480 K, whereas the contribution of the microcrystalline phase is weak. With the 20 wt% vanadia sample the contribution of the axial sites present at room temperature (Fig. 5b) disappears almost completely upon heating to 420 K (Fig. 5c) and the characteristic feature of the microcrystalline vanadium oxide becomes prevalent.

Slightly different behavior is observed with the 50 wt% vanadia sample (Figs. 5d and 5e). No indication is found for the presence of well-dispersed VO^{2+} ions. At lower temperatures (<390 K) this sample is made up predominantly of arrays of VO^{2+} species undergoing tumbling Brownian motion and the microcrystalline phase (Fig. 5d). When comparing the spectra shown in Figs. 5d and 5e, which were recorded at different temperatures, we note that in the temperature range 390–420 K most of the arrays of VO^{2+} species undergo agglomeration and finally form the microcrystalline phase.

Temperature-programmed reduction (TPR) was used to investigate the reducibility of the vanadia immobilized in the mixed gels. Figure 6 depicts the TPR profiles of the catalysts. Pure silica as well as the catalyst containing 0.1% vanadia did not exhibit any hydrogen consumption due to reduction. Two quantities were extracted from these profiles: (i) the ease of reduction of the vanadia, as reflected by the temperature of maximum reduction rate (T_{max}), and (ii) the fraction of reducible vanadia, as obtained from the measured hydrogen consumption and quantitative analysis by X-ray fluorescence. The changes of these

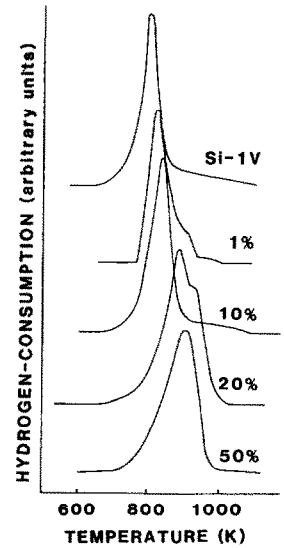

FIG. 6. TPR profiles of vanadia–silica mixed gels and silica-supported vanadia layer (Si–1V). Percentages quoted correspond to contents (wt%) of vanadia in mixed gels. TPR conditions are given in the Experimental section.

parameters as a result of the vanadia content of the catalysts are illustrated in Fig. 7.

The shift in T_{max} is most prominent between 10 and 20 wt% vanadia content. We also note that in this composition range the reduction peak becomes significantly broader and shows even a pronounced shoulder on the higher-temperature side (Fig. 6). This behavior is attributed to the occurrence of a smaller superimposed second reduction peak with higher T_{max} and indicates that in the catalysts containing more than 10–20 wt% vanadia a significant amount of a less easily reducible phase was present.

The reducible fraction of vanadia in the catalysts (Fig. 7) increased from about 40% for the catalyst containing 1 wt% vanadia to about 90% for the catalysts containing 50 wt% vanadia. Note that for the calculation of the vanadia species from the hydrogen consumptions it was assumed that reduction from V^{5+} to V^{3+} occurs. The error introduced in the determination of the reducible fraction by the fact that in the samples with high vanadia content some of the vanadia was present as V_3O_7 and V_6O_{13} was estimated to be less than 4%.

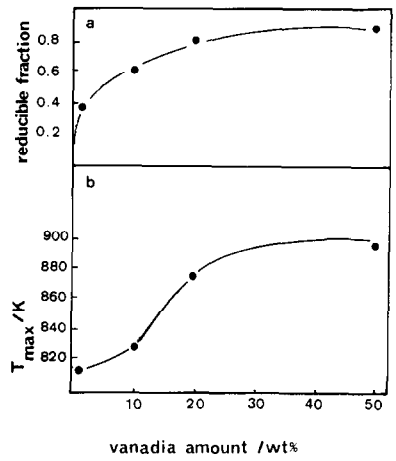

FIG. 7. Characteristic parameters derived from TPR measurements. (a) Reducible fraction of vanadia as determined from the hydrogen consumption and X-ray fluorescence measurements. (b) Ease of reduction of the vanadia in the mixed gels as reflected by the temperature of maximum hydrogen consumption (T_{max}).

4. Catalytic Activity

An analysis of possible interparticle and intraparticle heat transfer effects on our kinetic results (*17*) indicated that interphase and intraparticle temperature gradients could be neglected under the diluted gas conditions used (see under Experimental). In order to check for possible intraparticle mass transfer effects we performed a series of kinetic measurements with different vanadia–silica catalysts of 0.01- to 0.15- and 0.5- to 1-mm grain size and evaluated them by calculating the corresponding Damköhler numbers according to the procedure described in Ref. (*18*). The test series indicated that intraparticle diffusion limitations were unlikely under the conditions used for collecting the kinetic data.

Below 570 K all catalysts tested catalyzed selectively the reaction

$$NO + NH_3 + \tfrac{1}{4}O_2 \rightarrow N_2 + \tfrac{3}{2}H_2O$$

At higher temperatures N_2O was formed in addition to N_2, whereas NO_2 formation was never detected.

Both the overall activity and the specific activity were determined. The temperature (T_{50}) necessary to obtain 50% conversion of NO to N_2 under standard conditions was taken as a measure for the overall activity. The values measured for T_{50} were: pure silica, no activity; 0.1 wt% vanadia–silica, no activity; 1 wt% vanadia–silica, 504 K; 10 wt% vanadia–silica, 412 K; 20 wt% vanadia–silica, 456 K; and 50 wt% vanadia–silica, 391 K. Note that pure silica as well as 0.1 wt% vanadia–silica did not exhibit any activity under the conditions used.

The specific activity (specific reaction rate) was calculated as the number of moles of NO converted to N_2 per mole of V^{5+} per second. The number of V^{5+} species was calculated from the hydrogen consumption measured during TPR assuming that reduction from V^{5+} to V^{3+} occurred.

Figure 8 shows the dependence of the

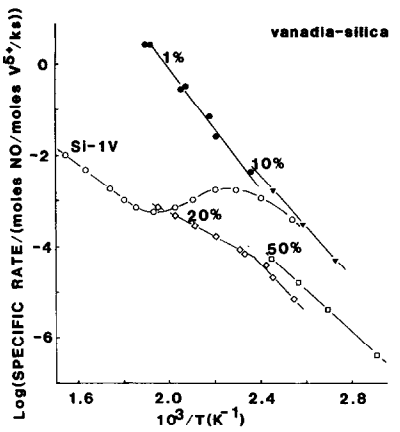

FIG. 8. Arrhenius plots of specific reaction rates for SCR measured over mixed gels of vanadia–silica and a silica-supported vanadia layer (Si–1V). Percentages denote contents (wt%) of vanadia in the mixed gels. Note that the mixed gel catalyst containing 0.1 wt% vanadia and pure silica did not exhibit significant activity under the conditions used.

specific reaction rates measured under the standard conditions quoted in the Experimental section. As mentioned above, silica and 0.1 wt% vanadia–silica were not active below 600 K. The silica-supported vanadia layer catalyst exhibited an activity curve with a maximum at 430 K and a minimum at about 510 K. This behavior was already reported elsewhere (*8*). It is interesting to note that the activity of the silica-supported vanadia layer at low temperatures was about the same as that measured for mixed gels with low amounts of vanadia. At higher temperatures, the silica-supported vanadia exhibited an activity similar to that of the mixed gels with high vanadia content.

DISCUSSION

1. Textural, Bulk Structural, and Chemical Properties

It has been shown that the textural properties of the vanadia–silica mixed gels depend strongly on their chemical composition (Table 1). The textural changes result from significant bulk structural changes which occur in this composition range.

Neither the XRD patterns (Fig. 2) nor the high-resolution electron micrographs (Figs. 3 and 4) give any indication of the presence of a crystalline phase in the fresh catalysts with low vanadia contents. Silica is present as a completely amorphous phase in all samples. Vanadia exhibits a more complex behavior. At low concentrations it forms an amorphous phase; i.e., there exists no distinct three-dimensional long-range ordering of the constituents. At higher vanadia concentrations (>10 wt%), some of the vanadia exists as small microcrystalline domains of V_3O_7 and V_6O_{13} which are embedded in the amorphous silica matrix.

More detailed bulk structural information emerges from the ESR investigations. The ESR spectra (Fig. 5) can be described as a superposition of the spectra due to three different paramagnetic VO^{2+} species: well-dispersed VO^{2+} ions, arrays of VO^{2+} species, and microcrystalline vanadium oxide. The latter phase exists as small microcrystalline domains embedded in the amorphous matrix as evidenced by HREM. The proportions of the different vanadium oxide species change with temperature. Higher temperatures favor the formation of the microcrystalline phase, probably due to the loss of adsorbed water and subsequent agglomeration of the VO^{2+} species. We note that the well-dispersed VO^{2+} species are considerably more stable in the samples with lower vanadia content. In these samples the VO^{2+} species are well separated by the silica matrix and consequently their agglomeration is suppressed.

Aldebert *et al.* (*19*) proposed that V_2O_5 gels consist of flat fibers crosslinked into layers. The fibers do not exhibit any orientation in the layer, but the distance of the layers is well defined and depends on the water content of the gel. With a decreasing amount of water the size of the coherence domain increases. Upon removal of the chemisorbed water above 623 K the V_2O_5 platelets are allowed to rearrange and crystallization occurs. Our investigations provide evidence that silica stabilizes the dis-

ordered V_2O_5 phase in the same way as the chemisorbed water does so in vanadia gels; i.e., it separates the vanadia layers or fibers and prevents them from coagulation and crystallization up to the calcination temperature of 873 K.

Temperature-programmed reduction (Figs. 6 and 7) revealed that this separation was complete for very low amounts of vanadia (0.1 wt%). In such samples practically no vanadia was accessible for reduction by hydrogen, suggesting that most of the vanadia was occluded by the silica matrix. This conclusion is further supported by the observed inactivity of these samples for SCR. With an increasing amount of vanadia the fraction of accessible and reducible vanadia increases strongly (Fig. 7) reaching about 90% when 50 wt% vanadia is present in the mixed gel.

The ease of reduction expressed as the temperature of maximum reduction rate (T_{max}) in the TPR profiles (Figs. 6 and 7) decreases with an increasing amount of vanadia. Above 10 wt% of vanadia the formation of a less easily reducible vanadium oxide phase is indicated by a second TPR peak at higher temperatures. This behavior is in line with the formation of microcrystalline domains of vanadium oxide observed by HREM (Fig. 4) in the catalysts containing 10 and more wt% vanadia and with the ESR results (Fig. 5) which indicate a trend toward an increase in the concentration of agglomerated vanadium oxide species with increasing vanadia concentration and temperature. It is interesting to note that the specific activity (Fig. 8) of the vanadia–silica decreases markedly when the second peak in the TPR profiles becomes dominant.

2. *Catalytic Activity*

The specific rates presented as turnover frequencies in Fig. 8 were based on the determination of the accessible V^{5+} sites by TPR. Thus the specific rates are based on the assumption that the V^{5+} sites accessible for hydrogen are equally well accessible for the reactants in SCR. This assumption is not necessarily valid. In any case the turnover frequencies represent conservative estimates, since some of the V^{5+} sites may be accessible for hydrogen but not for the reactant.

We note that highest specific rates were exhibited by the mixed gels containing 1 and 10 wt% of vanadia. The specific rate is significantly lower for the mixed gels containing 20 and 50 wt% vanadia, where part of the vanadia was existing as a microcrystalline phase. The transformation of parts of the amorphous vanadia into the microcrystalline phase observed with catalyst samples containing 10, 20, and 50 wt% vanadia results in a decrease in the specific rate. Note that both the 20 and the 50 wt% vanadia–silica catalysts exhibit a bend around 430 K in the Arrhenius plot (Fig. 8). The bend in the Arrhenius plot of the 50 wt% vanadia sample is not shown in Fig. 8, since under the conditions used complete conversion of NO was already obtained at lower temperatures. However, it could always be observed when the conditions were such that complete conversion was not obtained, e.g., when higher feed rates were applied.

The decrease in the activation energy with higher temperatures is attributed to the thermally induced agglomeration of the well-dispersed vanadia species, which leads to an increase in the fraction of the microcrystalline vanadium oxide phase in these samples.

We note that under the conditions where agglomeration did not occur, the activation energies of all catalysts were in the range of 42 ± 5 kJ/mol which is in good agreement with literature data (*20*).

The agglomeration of the well-dispersed vanadium oxide species under SCR conditions in the catalysts containing 20 and 50 wt% vanadia is supported by the results of the ESR investigations performed at different temperatures (Fig. 5). Thus it can be stated that the well-dispersed vanadium oxide species in the mixed gels with high

vanadia content (20 and 50 wt%) tend to agglomerate and then finally form microcrystalline domains at higher temperatures. Conversely, in the mixed gels containing low amounts of vanadia (<10 wt%), the well-dispersed vanadium oxide species remain stable even under reaction conditions due to their stabilization by the silica matrix which suppresses agglomeration.

Finally it is interesting to compare the activity behavior of the mixed gel catalysts with that of the silica-supported monolayer of vanadia, since this catalyst was found earlier (*8*) to undergo a structural transformation from well-dispersed vanadium oxide species at lower temperatures to microcrystalline vanadia at higher temperatures under SCR conditions.

We note that the low-temperature activity of the "monolayer" is about the same as the activity of the 1 wt% or the 10 wt% vanadia–silica mixed gel. However, at higher temperatures the activity dropped below the activity of the 20 wt% or the 50 wt% vanadia–silica mixed gel, indicating that the structural stability of the well-dispersed vanadium oxide species was in all mixed gels higher than that in the silica-supported monolayer of vanadia.

CONCLUSIONS

The sol–gel process is shown to be a method to modify the structural properties of a catalyst. It was possible to stabilize the structure of a vanadia gel by the addition of silica. The three-dimensional silica matrix prevents agglomeration and crystallization of the well-dispersed vanadia lamellae. A similar stabilization is not found for a vanadia layer immobilized on silica by the alkoxide route, due to the weak interaction of the vanadia with the silica surface. Silica-supported vanadia, when highly dispersed, tends to agglomerate, finally forming crystalline domains.

Mixed gels containing 1 to 10 wt% of vanadia were found to exhibit the highest specific activity for SCR. Higher contents of vanadia led to the formation of microcrystalline domains of vanadia. The microcrystalline vanadia was less easily reducible and exhibited a lower specific rate for SCR. The latter result provides further support for our earlier conclusion (*21*) that disordered vanadium oxide is considerably more active in SCR than crystalline vanadium oxide.

ACKNOWLEDGMENTS

Financial support by the Swiss National Science Foundation (project 2.020-0.83) and the "Schweizerischer Schulrat" is gratefully acknowledged.

REFERENCES

1. Haber, J., Kozowska, A., and Kozowski, R., *J. Catal.* **102,** 52 (1986).
2. Roozeboom, F., Mittelmeijer-Hazeleger, M. C., Moulijn, J. A., Medema, J., de Beer, V. H. J., and Gellings, P. J., *J. Phys. Chem.* **84,** 2783 (1980).
3. Murakami, Y., Inomata, M., Mori, K., Ui, T., Suzuki, K., Miyamoto, A., and Hattori, T., *in* "Preparation of Catalysts, III" (G. Poncelet, P. Grange, and P. A. Jacobs, Eds.), Stud. Surf. Sci. Catal., Vol. 16, p. 531. Elsevier, Amsterdam, 1983.
4. Kijenski, J., Baiker, A., Glinski, M., Dollenmeier, P., and Wokaun, A., *J. Catal.* **101,** 1 (1986).
5. Ueno, A., Todo, N., Kurita, M., Hagiwara, H., Nishijama, A., Sato, T., and Kiyozumi, Y., *Chem. Lett.*, 557 (1979).
6. Shikada, T., Fujimoto, K., Kunugi, M., and Tominaga, H., *J. Chem. Technol. Biotechnol. A* **33,** 446 (1983).
7. Takagi, M., Soma, M., Onishi, T., and Tamaru, K., *Canad. J. Chem.* **58,** 2132 (1980).
8. Baiker, A., Dollenmeier, P., Glinski, M., and Reller, A., *Appl. Catal.* **35,** 365 (1987).
9. Pierce, C., *J. Phys. Chem.* **57,** 149 (1953).
10. Monti, D., and Baiker, A., *J. Catal.* **83,** 323 (1983).
11. Baiker, A., Dollenmeier, P., and Reller, A., *J. Catal.* **103,** 394 (1987).
12. Gude, A. J., and Sheppard, R. A., *Amer. Mineral.* **57,** 1053 (1972).
13. Walterson, K., Forslund, B., Wilhelmi, K. A., Anderson, S., and Galy, J., *Acta Crystallogr. B* **30,** 2644 (1974).
14. Wilhelmi K. A., Walterson, K., and Kihlborg, L., *Acta Chem. Scand.* **25,** 2675 (1971).
15. Tounge, P., Legrand, A. P., Sanchez, S., and

Livage, J., *J. Phys. Chem. Solids* **42,** 101 (1981); Sanchez, S., Livage, L., Tounge, P., and Legrand, A. P., *Magn. Reson. Colloid Interface Sci.* **2,** 559 (1979).

16. Sharma, V. K., Wokaun, A., and Baiker A., *J. Phys. Chem.* **90,** 2715 (1986).
17. Dollenmeier, P., Ph.D. thesis, No. 8241, ETH, Zürich, 1987.
18. Anderson, J. R., and Pratt, K. C., "Introduction to Characterization and Testing of Catalysts," p. 268 et seq. Academic Press, London, New York, 1985.
19. Aldebert, P., Baffier, N., Gharbi, N., and Livage, J., *Mater. Res. Bull.* **16,** 669 (1981).
20. Bauerle, G. L., Wu, S. C., and Nobe, K., *Ind. Eng. Chem. Prod. Res. Dev.* **17,** 117 (1978); Inomata, M., Miyamoto, A., and Murakami, Y., *J. Catal.* **62,** 140 (1980).
21. Baiker, A., Dollenmeier, P., Glinski, M., and Reller, A., *Appl. Catal.* **35,** 351 (1987).